RSC Advances

ROYAL SOCIETY OF CHEMISTRY

www.rsc.org/advances

Journal Name

RSCPublishing

ARTICLE

Wool graft polyacrylamidoxime as the adsorbent for adsorption both cationic and anionic toxic ions from aqueous solutions†

Cite this: DOI: 10.1039/x0xx00000x

Received 00th January 2012,
Accepted 00th January 2012

DOI: 10.1039/x0xx00000x

www.rsc.org/

Chun Cao,[a,b] Hongliang Kang,*[a] Ning Che,[a,b] Zhijing Liu,[a,b] Pingping Li,[a,b] Chao Zhang,[a,b] Weiwei Li,[a,b] Ruigang Liu*[a] and Yong Huang*[ac]

Wool graft polyacrylamidoxime (W-*g*-PAO) was synthesized using coarse wool as the raw keratin material and the graft polymerization parameters were optimized. The adsorption properties of W-*g*-PAO for both cationic and anionic toxic ions from aqueous solutions were investigated. It was found that both cationic and anionic toxic ions can be effectively adsorbed by W-*g*-PAO. The adsorption followed the pseudo-second-order kinetics model for both cations and anions, and can be well depicted by Langmuir isotherm model. The equilibrium adsorption capacity (Q_e) increases with the rising initial concentration of toxic ions. The adsorption capacity followed the order of Hg^{2+} > Pb^{2+} > AsO_2^- > AsO_4^{3-} > Cd^{2+}. W-*g*-PAO can be regenerated after adsorption, and the adsorption capacity slightly decreased with the increase in the regenerated cycles. Besides providing a cheap and excellent adsorbent for the removal of both cationic and anionic toxic ions from waste water, the method can be extended to the modification of other waste raw keratin materials, by which the waste raw keratin materials can be used as a valuable blocks for the fabrication of functional materials.

1. Introduction

Toxic ions, including cations (e.g. Cd^{2+}, Hg^{2+}, Pb^{2+}, Cu^{2+}) and anions (CrO_4^{2-}, AsO_4^{3-}, AsO_3^- F^-), are not biodegradable and tend to accumulate in living organisms, causing a number of health problems, diseases and disorders.[1] These toxic ions generally exist in aqueous waste from industries of metal plating, electronics, mining activities, etc.[2,3] and even ground water in some cases. The removal of toxic ions from polluted water is an urgent issue, which can be achieved by chemical precipitation,[4-6] membrane filtration,[7,8] reverse osmosis,[9-11] ion-exchange,[12,13] and adsorption.[14,15] The adsorption method using adsorbents is the attractive one due to its easy operation.[14-16] An idea adsorbent should have the characteristics of containing desired functional groups, high specific surface area, reusable, and cheap. The desired functional groups for heavy metal ion adsorption are generally containing electron-rich heteroatoms, such as nitrogen, oxygen, sulphur, phosphorus, by which chemical bond with the heavy metal ions can be formed for immobilizing the metal ions.[17-19] Adsorbents of different matrix and functional groups have been investigated extensively.[20-25] However, the cost of the adsorbents is still the main issue that limits the wide applications.[16]

Keratin is the structural protein in feather, hair, wool, horn, nails etc. and is renewable and biocompatible. Keratin contains abundant cysteine residues that form permanent and thermal stable disulfide bridges to stabilized the structure of keratin.[26] Nowadays, only a few keratin wastes have been hydrolysed to peptides and amino acid and used as additives in cosmetics.[27] Some works focused on the functional biomaterials with keratin as building blocks for the applications in tissue engineering and drug delivery.[28-31] However, most of the raw keratin materials are discarded as the waste by-products of various industries, which cause environmental pollution.[32-34] Considering the high output of raw keratin materials ever year in the world, it is urgent to investigate the functionalization and applications of the valuable raw keratin as the blocks of functional materials. Wool waste is one of the represented raw keratin materials, which is cheap, abundant and attainable in slaughter-house,

[a]*Sate Key Laboratory of Polymer Physics and Chemistry, Beijing National Laboratory of Molecular Sciences, Institute of Chemistry, Chinese Academy of Sciences, Beijing 100190, China. E-mail: rgliu@iccas.acn, Fax & Tel: +86-10-82618573*

[b]*University of Chinese Academy of Science, Beijing, 100049, China*

[c]*Natural Research Center for Engineering Plastics, Technical Institute of Physics & Chemistry, Chinese Academy of Sciences, Beijing 100190, China*

† Electronic supplementary information (ESI) available. The optimization of the synthesis of W-*g*-PAO, and the adsorption data for properties of Cu^{2+}, Hg^{2+}, Pb^{2+}, and AsO_2^-. See DOI: 10.1039/x0xx00000x

textile industries (coarse and/or short wool), and even the used wool fabrics.[35]

According to the amino acid sequence, keratin has about 40% hydrophilic chemical groups and 60% hydrophobic chemical groups in its structure. The cheap and abundant wool waste has the great potentials for being used as one of the low cost adsorbent. Recently, keratin based materials have been used for the adsorption of heavy metal cations from waste water.[36-39] However, the inherent functional groups of the wool keratin were mainly used to adsorb the toxic ions. The introduction of new functional groups to the surface of the keratin materials could improve the adsorption ability for being used as the adsorbent for removal heavy metal ions from waste water. Surface graft modification has been investigated extensively to improve the properties of wool fabrics.[40-44] The success of the surface graft modification is mainly due to the mercapto groups in wool reduced from disulfide bonds, which serve as the chain transfer active sites of the free radical polymerization.

Amidoxime group has the strong chelating ability for heavy metal ions.[45-47] In this work, coarse wool was used as the raw keratin materials. Wool surface graft polyacrylonitrile (W-*g*-PAN) was first synthesized and the cyano groups were then converted into amidoxime groups to result the wool surface graft polyacrylamidoxime (W-*g*-PAO). The parameters for the surface graft modification were optimized and the adsorption properties for toxic cations and anions such as Cd^{2+}, Pb^{2+}, Hg^{2+}, AsO_4^{3-}, and AsO_2^- from aqueous solution were investigated.

2. Experimental section

2.1. Materials

Coarse wool from the wool industry was kindly supplied by Erdos Group (Inner Mongolia, China). The lanolin on the surface of wool was washed by immersing the wool in acetone for 24 h. The wool was then immersed in NaOH (0.5 wt%) and Na_2S (0.5 wt%) mixed aqueous solution for 5 min to reduce disulfide bonds to mercapto groups, after which washed with deionized water and vacuum dried at 35 °C. The dried wool was stored in inert atmosphere before use.

$Cd(NO_3)_2$, $Hg(Ac)_2$, $Pb(NO_3)_2$, $CuSO_4$, Na_3AsO_4, $NaAsO_2$, and hydroxylamine hydrochloride were supplied by Sinopharm Company of China. α,α'-Azodiisobutyramidine dihydrochloride (V50) was purchased from Aladdin Industrial Inc., China). Acrylonitrile (Beijing Chemical Plant) was flow through the column packed with basic alumina to remove trace inhibitor before use. All the other solvents and chemicals were supplied by local chemical suppliers and used as received.

2.2. Synthesis of W-*g*-PAO

The synthesis route of W-*g*-PAO is shown in Fig. 1. Typically, the activated dried wool (2.5 g) was immersed in urea solution (8 M, 150 mL) and the mixture was bubbling with N_2 and stirring at 50 °C for 30min. After dissolving V50 (0.216 g) in the reaction mixture, the reaction mixture was then heated to 65 °C, during which acrylonitrile (20 mL) was added dropwise with continuously stirring and bubbling with N_2. The reaction vessel was sealed and kept at 65 °C for another 12 h to result W-*g*-PAN. The crude W-*g*-PAN was washed with DMSO, deionized water and acetone for several times to remove free PAN and other impurities. The W-*g*-PAN was dried in vacuum at 40 °C. PAN content (G_d) in W-*g*-PAN was determined by $G_d(\%)=(W_1-W_0)/W_0\times100$, where$W_0$ and W_1 are the mass of wool before and after the graft polymerization, respectively.

The conversion of cyano groups into amidoxime groups has been reported in details in previous work.[48] Briefly, W-*g*-PAN (1.0 g) was treated with the mixed solution of NaOH (1.0 mol L^{-1}, 100 mL) and $NH_2OH{\cdot}HCl$ (1.0 mol L^{-1}, 100mL) at 65 °C for 6 h with continuously stirring. The product was washed with distilled water and then acetone for several times to result W-*g*-PAO. The resultant materials were vacuum dried at 40 °C and stored for characterization and adsorption experiments.

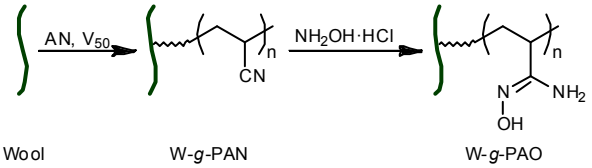

Fig. 1 The synthetic route of W-g-PAO.

2.3. The adsorption of toxic ions by W-*g*-PAO

The adsorption kinetics and the influence of pH, concentration were investigated. Solutions with desired concentration of Cd^{2+}, Pb^{2+}, Hg^{2+}, Cu^{2+}, AsO_4^{3-} and AsO_2^- ions were prepared. W-*g*-PAO (0.20 g) was immersed in the solutions (200 mL) with desired concentrations of toxic ions for 24 h at 25 °C, during which the concentration of toxic ions was measured by inductively coupled plasma atomic emission spectroscopy (ICP-AES). For prevention forming insoluble metal hydroxides, the pH of the solutions for adsorption kinetics experiments was kept at 5.6, 4.8, and 6.0 for Cd^{2+}, Hg^{2+}, and Pb^{2+}, respectively. The adsorption kinetics of W-*g*-PAO for Cd^{2+}, Hg^{2+}, and Pb^{2+} in aqueous solutions (10 mg L^{-1}) was investigated in the pH range of 2–6. The adsorption kinetics of W-*g*-PAO for AsO_4^{3-} and AsO_2^- in aqueous solutions (10 mg L^{-1}) was investigated in the pH range of 2–12.The toxic ions absorbed by W-*g*-PAO at time t, Q_t (mg g^{-1}), and the adsorption capacity of toxic ions by W-*g*-PAO at equilibrium state, Q_e, (mg g^{-1}), were calculated by,

$$Q_t = \frac{(C_0 - C_t)V_s}{m} \quad (1)$$

$$Q_e = \frac{(C_0 - C_e)V_s}{m} \quad (2)$$

where, C_0, C_t, and C_e are the concentration (mg L^{-1}) of toxic ions at the initial state, at time t, and at the equilibrium state, respectively. V_S is the volume (L) of the ion solution and m is the mass (g) of W-*g*-PAO. The content of W-*g*-PAO was kept

at 1.0 g L^{-1} in all the adsorption experiments.

The adsorption-desorption experiments were carried out as follows. W-*g*-PAO (0.20 g) was immersed in solutions (200 mL) of heavy metal ions (20 mg L^{-1} of Cd^{2+}, Pb^{2+}, Hg^{2+}) and stirred at 25 °C for 24 h. The adsorbent W-*g*-PAO was then dried and then immersed in saturated EDTA solution (20 mL) at 25 °C for desorption. The EDTA solution was replaced every 12 h for 5 times, after which W-*g*-PAO was washed with deionized water and dried for another cycle. The adsorption-desorption was carried out for 5 cycles. The concentration of heavy metal ions solutions was detected by ICP-AES.

2.4. Characterization

Fourier transform infrared spectroscopy (FTIR) was carried out on a Bruker-Equinox 55 FTIR spectrometer (Germany). Element analysis was performed on A Flash EA 1112 elemental analyser (Thermo scientific, USA). Scanning electron microscope (SEM) observation was carried out on a Hitachi S-4300 SEM (Japan) operating at 3.0 kV. The content of heavy metal ions was measured on an inductively coupled plasma atom emission spectrometer (ICP-AES, Thermo scientific, USA). The pH of the solution was detected by an Orion Star A211 pH meter (Thermo scientific, USA).

3. Results and discussion

3.1. Synthesis and characterization of W-g-PAO

The synthesis of W-*g*-PAO was carried out according two-step approach (Fig. 1). The reaction conditions including reaction solvent, reaction temperature, initiator dose, and monomer dose for the synthesis of W-*g*-PAN were first optimized. The experimental details and the resulted W-*g*-PAN are listed in Table S1, by which the optimum reaction conditions were selected as follows. Urea solution (8 M) was selected as the reaction medium, the reaction temperature was set at 65°C, and the reactions were performed for 12 h. The content of PAN in W-*g*-PAN can be adjusted by changing the feeding ratio of the monomer acrylonitrile (AN) to wool in the reaction mixture. Hereafter the content of amidoxime groups in the resulted W-*g*-PAO can be adjusted. In the following experiments, W-*g*-PAN with the PAN content (G_d) of 54.20% was selected as the typical material.

The success of the graft PAN onto wool surface and the conversion of PAN to PAO were estimated by FTIR. Fig. 2 shows the FTIR spectra of wool, W-*g*-PAN, and W-*g*-PAO. The characteristic absorbance band of cyano groups appeared at 2243 cm^{-1} in the FTIR spectrum of W-*g*-PAN (Fig. 2b), which confirmed success of the graft copolymerization of PAN onto the wool surface. After the amidoximization, the absorbance band of cyano groups at 2243 cm^{-1} totally disappeared (Fig. 2c). Meanwhile, new bands at 911 and 1388 cm^{-1} appear on the FTIR spectrum of W-*g*-PAO, corresponding to the N–O stretching and O–H bending vibrations of the amidoxime groups. In addition, three new absorbance bands appeared at 3464, 3315, and 3183 cm^{-1}, which attribute the stretching vibration of O–H and N–H. FTIR spectra confirmed the complete conversion of cyano groups to amidoxime groups and the successful synthesis of W-*g*-PAO. The morphology of the wool and the corresponding surface graft modified wool was observed by SEM and polarized optical microscopy (POM). The results indicate that the morphology of the wool was kept during the graft reactions (Fig. S1). Elemental analysis results of wool, W-*g*-PAN, and W-*g*-PAO are listed in Table 1. The N/C mole ratio of wool, W-*g*-PAN, and W-*g*-PAO is 0.286, 0.312, and 0.443, respectively. The higher N/C mole ratio of W-*g*-PAN and W-*g*-PAO confirmed the graft of PAN and hereafter conversion of PAN to PAO.

Table 1 Elemental analysis of activated wool, PAN, W-*g*-PAN, W-*g*-PAO.

Sample	Composition (wt%)			N/C (mole ratio)
	C	N	H	
wool	45.28	15.08	6.66	0.286
PAN	66.85	25.35	5.31	0.325
W-*g*-PAN	54.79	19.96	6.28	0.312
W-*g*-PAO	42.13	21.76	7.06	0.443

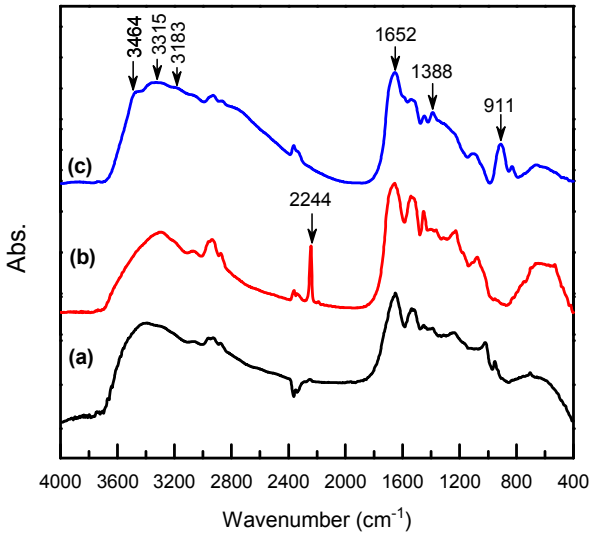

Fig. 2 The FTIR spectra of (a) wool, (b) W-*g*-PAN, and (c) W-*g*-PAO.

3.2. The adsorption of toxic ions by W-g-PAO

The adsorption of W-g-PAO was first checked using Cu^{2+} by the immersing the wool, W-*g*-PAN, and W-*g*-PAO samples in $CuSO_4$ aqueous solution (Fig. S2, ESI). The photos of the dried samples are also shown in the last column. The results show that the colour of the wool and W-*g*-PAN samples only becomes light blue after the adsorption. While the W-*g*-PAO sample become deep blue and finally dark blue and the dried sample is in black colour. The results indicated that the W-*g*-PAO samples have the good adsorbing ability for Cu^{2+} cations, which is due to that the amidoxime groups graft on the surface of the wool have the strong chelating ability for cations.[45-47]

The adsorption kinetics of W-*g*-PAO for Cu^{2+}, Cd^{2+}, Pb^{2+}, Hg^{2+}, AsO_4^{3-}, and AsO_2^- at different initial concentration of the toxic ions was investigated. The results of Cd^{2+} and AsO_4^{3-} are shown in Fig. 3 for representing the adsorption of toxic cations and anions, respectively. Other data are shown in Fig. S3 (ESI). For the adsorption of heavy metal cations, the adsorption rate is quite fast within the first hour (Fig. 3a), which attributes to the abundant active sites in the adsorbent. For solutions with low heavy metal ions, e.g. in Cd^{2+} solution of 3.8 mg L^{-1}, the cations adsorbed by W-*g*-PAO levelled off within one hour, which is due to that the Cd^{2+} ions, totally 0.76 mg Cd^{2+} solution (200 mL) was almost all adsorbed by W-*g*-PAO (0.72 mg). With the increase in the concentration of Cd^{2+} ions, the adsorbed Cd^{2+} ions on W-*g*-PAO rises accordingly (Fig. 3a). For the solution with relatively higher heavy metal cations, the fast adsorption finished within 2 h and then levelled off. A higher initial toxic ion concentration correlates a faster adsorption rate and a higher adsorption capacity of toxic ions at the equilibrium state, which is due to the higher chelating ability of the toxic metal ions of the amidoxime groups. The absorption of toxic anions, e.g. AsO_4^{3-}, is slightly different compared with that of cations. There is a fast adsorption step, which finished within about 15 min, then the adsorbed AsO_4^{3-} increases slowly with the adsorption time (Fig. 3b). The adsorption ability for AsO_4^{3-} is comparable to that of Cd^{2+}. The adsorption behaviour for Cu^{2+}, Pb^{2+}, Hg^{2+}, and AsO_2^- are similar to those of the Cd^{2+} and AsO_4^{3-} toxic ions.

The kinetics and isotherm of the adsorption can be depicted by the pseudo second order kinetics. The saturated adsorption capacity of adsorbent for toxic ions can be estimated by using the isotherm Langmuir model,

$$\frac{t}{Q_t} = \frac{t}{Q_e} + \frac{1}{K_1 Q_e^2} \quad (3)$$

$$\frac{C_e}{Q_e} = \frac{C_e}{Q_0} + \frac{1}{Q_0 K_L} \quad (4)$$

where t is the contact time of adsorption procedure, Q_t and Q_e are the adsorbed toxic ions on the adsorbent at adsorption time t and at equilibrium state, which were calculated by using Eqs. 1 and 2. K_1 and K_L are the adsorption rate constant of the pseudo-second-order kinetics model and the adsorption equilibrium constant in Langmuir model, respectively.

Generally, a linear fit of the pseudo-second order model is used for the fitting of the experimental data to obtain the kinetic parameters. The results of the linear fit of the pseudo-second order model are apparently perfect, as shown in Fig. S4 and Table S3 (ESI) for fitting results of present work. However, the linearization of the original data will change the error distribution, which is not as beautiful as it appearance. The non-linear fitting method is actually a better way to obtain kinetic parameters.[49-52] In this work, the non-linear fitting of pseudo-first (Eq. S1, ESI) and pseudo-second order (Eq. 3) models have been used for fitting the experimental data. The fitting curves and the correlation coefficient R^2 by using different models are presented in Figs. S5 and S6 and Tables S4 and S5 (ESI). The comparison of the correlation coefficient R^2 in Tables S4 and S5 (ESI) indicates that the nonlinear fit of pseudo-second order model as described in Eq. 3 is better to obtain kinetic parameters of the adsorption in present work. Q_e was calculated by fitting the adsorption data using the nonlinear fitting using Eq. 3 and C_e was calculated by using Eq. 2. The results are listed in Table 2.

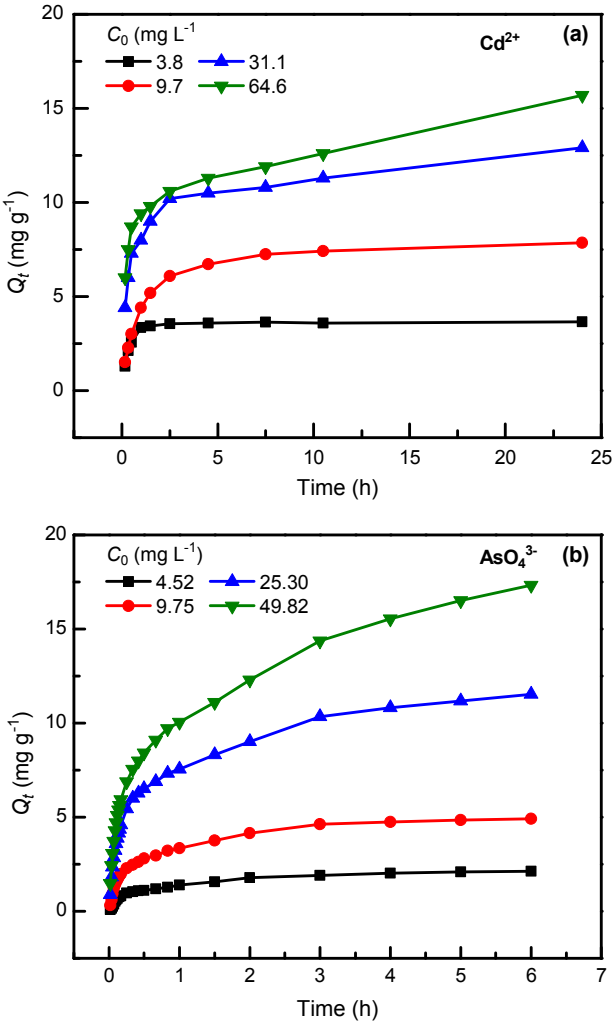

Fig. 3. The adsorption kinetics of (a) Cd^{2+} and (b) AsO_4^{3-} ions from water by W-*g*-PAO at different initial concentration.

Fig. 4a shows the dependence of the initial concentration of toxic ions (C_0) on the equilibrium adsorption capacity (Q_e). The results show that Q_e increases with the rising initial concentration of the toxic ions in all the cases. Specifically, Q_e of Hg^{2+} nearly increases linearly with the rising initial concentration and almost all of Hg^{2+} can be removed by using the adsorbent when the initial concentration of Hg^{2+} is lower than 50 mg L^{-1} in present work. However, for Cd^{2+}, AsO_2^- and AsO_4^{3-}, the Q_e increases slowly with the rising C_0. The adsorption capacity followed the order of Hg^{2+}>Pb^{2+}>AsO_2^-> AsO_4^{3-}>Cd^{2+}.

Table 2. The Q_e and C_e obtained from the adsorption experiments.[a]

Cd^{2+}			Hg^{2+}			Pb^{2+}			AsO_4^{3-}			AsO_2^-		
C_0	Q_e	C_e	C_0	Q_e	C_e	C_0	Q_e	C_e	C_0	Q_e	C_e	C_0	Q_e	C_e
3.80	3.8	0	6.83	6.8	0.03	1.50	1.42	0.08	4.52	2.10	2.42	10.5	4.0	6.5
9.70	8.0	1.7	18.8	18.6	0.2	4.20	4.10	0.10	9.75	4.80	4.95	24.7	8.0	16.7
31.1	11.5	19.6	24.4	23.6	0.80	15.5	14.0	1.50	25.3	10.7	14.6	34.3	9.7	24.6
64.6	12.9	51.7	53.5	41.2	12.3	38.8	21.8	17.0	49.8	15.8	34.0	53.1	15.4	37.7

[a] The units for C_0, Q_e, and C_e are mg L^{-1}, mg g^{-1}, and mg L^{-1}, respectively.

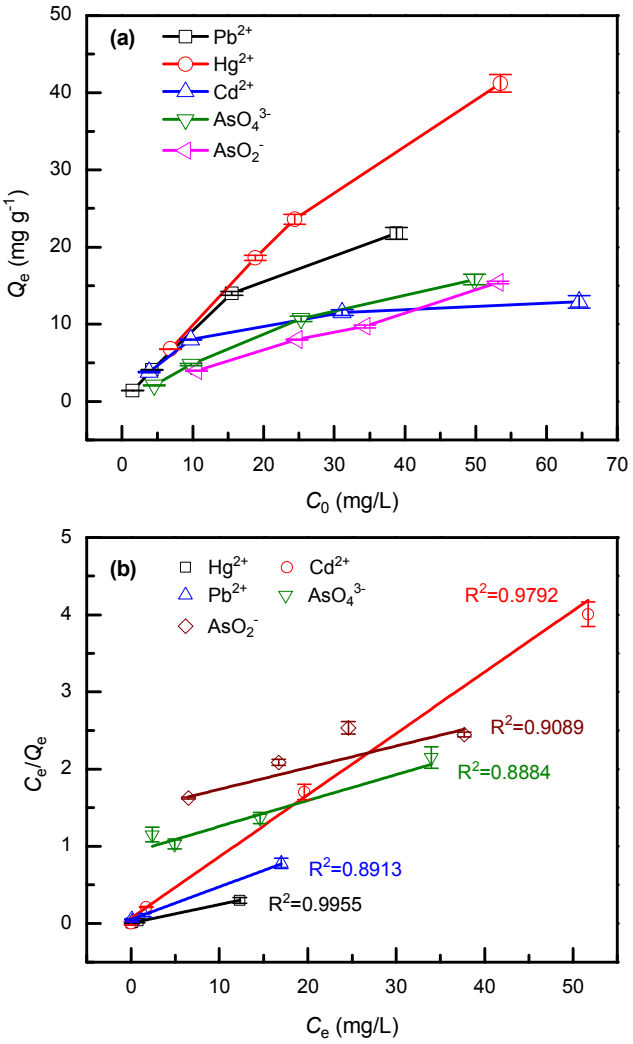

Fig. 4. The influence of initial concentrations of toxic ions (C_0) on the equilibrium adsorption capacity (Q_e) (a) and the adsorption isotherms fitted by Langmuir model as descripted in eq. 4 (b).

Fig. 4b shows the adsorption isotherms of adsorption experiments that fitted by Langmuir model using the data listed in Table 2. The data were also fitting by Freundlich and Temkin models for comparison (Fig. S7, ESI) and the R^2 obtained by fitting the experimental data using different adsorption isotherm models for the toxic ions are listed in Table S6 in ESI. The results indicated that Langmuir model is the best model for fitting the experimental data. In Fig. 4b, several data points of Hg^{2+} and Pb^{2+} ions are close to each other at low C_e, which is due to that the W-*g*-PAO adsorbent has the strong adsorption capacity for Hg^{2+} and Pb^{2+} cations. For clarification, Fig 4b was also depicted in semi-log plot in Fig. S8 (ESI).

According to Langmuir model, the saturated adsorption capacity (Q_0) of the toxic ions of the adsorbent could be obtained, Q_0 is 12.55, 23.56, 41.53, 29.78, and 35.52 mg g^{-1} for Cd^{2+}, Pb^{2+}, Hg^{2+}, AsO_4^{3-} and AsO_2^-, respectively. The saturated adsorption capacity of W-*g*-PAO is much higher than some other low-cost biomaterials adsorbents reported in literatures. The Q_0 for ploy(methacrylate) modified cellulose acetate membrane is 3.31 and 23.08 for Cd^{2+} and Hg^{2+}, respectively.[53] And Q_0 for sporopollenin is 4.37 and 1.64 mg g^{-1} for Pb^{2+} and Cd^{2+} ions, respectively.[54] Besides, due to the lower the specific surface area of W-*g*-PAO, the adsorption capacities of W-*g*-PAO is lower than those adsorbents with nanostructure. For example, the Q_0 for SCNCs is 367 and 259 mg g^{-1} for Cd^{2+} and Pb^{2+}, respectively.[1]

3.3. Influence of pH on the adsorption for cations and regeneration of the adsorbent

Fig. 5 shows the influence of pH on adsorption capacity of different heavy metal ions. For the cations (Fig. 5a), the adsorption capacity of Cd^{2+} and Pb^{2+} decreased rapidly in the range of pH < 4.0. However, while the adsorption capacity of Hg^{2+} ions only changed slightly within the pH range of 2.0–5.0. The results also demonstrated clearly that the optimal adsorption pH value for Cd^{2+}, Pb^{2+} and Hg^{2+} are 5.0, 4.8, and 3.9, respectively. On the contrary, the equilibrium adsorption capacity (Q_e) for AsO_4^{3-} and AsO_2^- is almost independent on the pH in the pH range of 2.0–9.0. However, Q_e decreases slightly with the increase in pH at pH > 9.0 (Fig. 5b). The results suggest that W-*g*-PAO has good adsorption properties for AsO_4^{3-} and AsO_2^- in a wide pH range.

The adsorption mechanism of W-*g*-PAO for cationic and anionic toxic ions can be depicted schematically in Fig. 6. For the adsorption of cations, the amidoxime groups on W-*g*-PAO contain strong nucleophilic $-NH_2$ and =N–OH groups and have the strong chelating ability for heavy metal ions,[45-47] such as Cu^{2+}, Cd^{2+}, Hg^{2+}, and Pb^{2+} in this work (Fig. 6a). At low pH, the $-NH_2$ groups will be protonated to form $-NH_3^+$ cations. Therefore, the adsorption of cations decreased with the

decrease in the pH of the media (Fig. 6a), which is due to the electrostatic repulsion between the $-NH_3^+$ and metal cations (Fig. 6b). The adsorption of anions, such as AsO_4^{3-} and AsO_2^- in present work, by W-*g*-PAO is in a different way. The status of AsO_4^{3-} depends on redox potential and pH. In oxidising condition, $H_2AsO_4^-$ is dominant at the pH less 6.9, whilst $HAsO_4^{2-}$ is dominant at higher pH. In reducing conditions, the uncharged arsenite $HAsO_2{\cdot}H_2O$ is dominant at pH < 9.2.[55] The amidoxime groups in of on W-*g*-PAO offer the reducing environment,[48] at least on the surface of the absorbent. Therefore, it is reasonable that the AsO_4^{3-} anions could be reduced into $HAsO_2{\cdot}H_2O$ form at low pH. The hypothesis suggests that the adsorption of AsO_4^{3-} and AsO_2^- should in the similar way by W-*g*-PAO at low pH. For clarification, the adsorption data AsO_4^{3-} in Fig. 5b was converted to the mass of AsO_2^- of the same mole that adsorbed on W-*g*-PAO, and the data are shown in Fig. 5b (calculated). The calculated data are similar with the adsorption data of AsO_2^-, which confirm that AsO_4^{3-} has been converted into AsO_2^- at low pH in this work. The adsorption of AsO_2^- can be adsorbed by electrostatic attraction at low pH (pH < 9.0) by using W-*g*-PAO as the adsorbent (Fig. 6c). At higher pH, the de-protonation of $-NH_3^+$ will lead the decrease in the electrostatic attraction and the adsorption of both AsO_4^{3-} and AsO_2^- (Fig. 5b). The adsorption capacity of AsO_4^{3-} by the W-*g*-PAO is around 5.0 mg g^{-1}, which is high than that of polyethylene polyamine modified cellulose pulp (about 2.0 mg g^{-1}).[56]

In practical application, the reusing of adsorbents is vital to cut down the cost. Therefore, the cycle efficiency of W-*g*-PAO was tested. Fig. 7 shows the cycle efficiency of W-*g*-PAO, the adsorption capacity of the adsorbent for Cd^{2+} and Pb^{2+} decreases gradually after cycled for several times, which is probably attribute to the losing of active sites during the desorption. However, the Q_e of Hg^{2+} keeps at a high value, which is due to the high adsorption capacity of Hg^{2+} on W-*g*-PAO. And in spite of losing some active sites, the ones left are still more than enough to adsorb almost all Hg^{2+}. In detail, the total lose in adsorption performance were 27% for Cd^{2+}, 29% for Pb^{2+} and only 5% for Hg^{2+} after five adsorption/desorption cycles. The morphology of W-*g*-PAO remains unchanged during the recycling procedure.

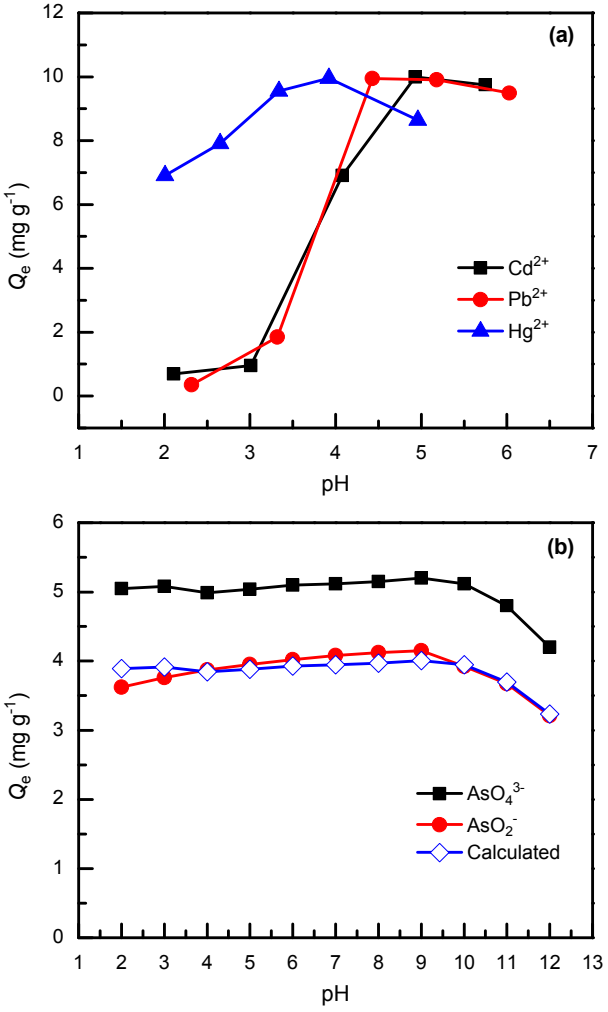

Fig. 5. The influence of pH value on adsorption capacity. The initial concentration of the cations was kept at 10 mg L^{-1}.

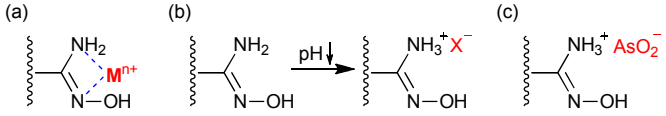

Fig. 6. (a) The adsorption of heavy metal cations by amidoxime groups on W-g-PAO, (b) the protonation of $-NH_2$ groups, and (c) the adsorption of AsO_2^- anions by W-g-PAO through the electrostatic attraction between protonated $-NH_3^+$ and AsO_2^- ions.

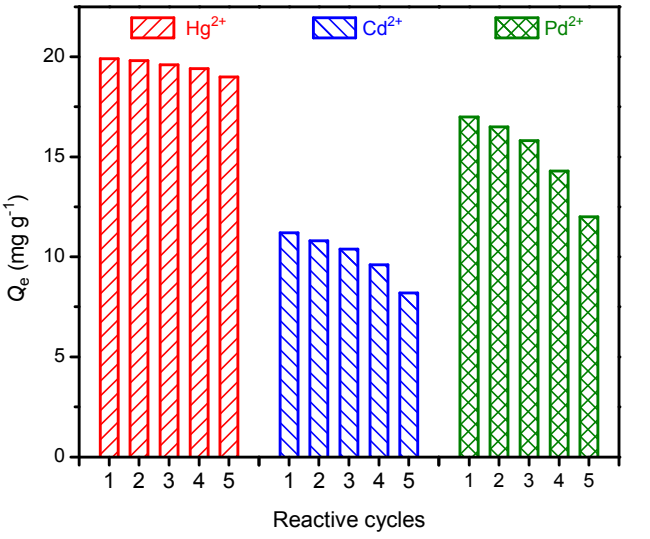

Fig. 7. The regeneration properties of W-*g*-PAO. The initial concentration of the toxic cations was kept at 20 mg L^{-1} for the adsorption experiments.

The above results and discussions confirmed that coarse wool can be modified via simply surface graft polymerization. The resultant W-*g*-PAO can be used as the adsorbent for adsorbing both cationic and anionic toxic ions from waste water. The results in this work provide a cheap and excellent adsorbent that can be used for the removal of both cationic and anionic toxic ions from waste water. Besides the raw keratin material, coarse wool, used in this work, the approach in this work can be extended to the modification of any other waste raw keratin materials, by which the waste raw keratin materials can be used as a valuable blocks for the fabrication of functional materials.

4. Conclusions

Coarse wool waste was modified by surface grafting of polyacrylonitrile (W-*g*-PAN) and then converting the cyano groups to amidoxime groups to result wool surface graft polyacrylamidoxime (W-*g*-PAO). The reaction parameters for the synthesis of W-*g*-PAO were optimized. Adsorption experiments indicated that W-*g*-PAO can effectively adsorb both cationic and anionic toxic ions from waste water. The adsorption followed the pseudo-second-order kinetics model for both cations and anions, and can be well depicted by Langmuir isotherm model. The equilibrium adsorption capacity (Q_e) increases with the rising initial concentration of toxic ions. The adsorption capacity followed the order of $Hg^{2+} > Pb^{2+} > AsO_2^- > AsO_4^{3-} > Cd^{2+}$. At pH < 4.0, the adsorption ability for Pb^{2+} and Cd^{2+} decreased dramatically, while the adsorption ability for Hg^{2+} changed slightly in the pH of 2.0–6.0. The adsorption ability kept at constant in the pH range 2.0–9.0 for both AsO_4^{3-} and AsO_2^-. W-*g*-PAO can be regenerated after adsorption, and the adsorption capacity slightly decreased with the increase in the regenerated cycles. The present work provided an approach for using the waste raw keratin materials as the valuable blocks for the fabrication of functional materials.

Acknowledgements

This work was supported by the National Natural Science Foundation of China (21174150 and 21174156) and National Program on Key Basic Research Project of China (973 Program) (2011CB605604).

References

1. X. L. Yu, S. R. Tong, M. F. Ge, L. Y. Wu, J. C. Zuo, C. Y. Cao and W. G. Song, *J. Environ. Sci.*, 2013, 25, 933-943.
2. F. Ji, C. Li, B. Tang, J. Xu, G. Lu and P. Liu, *Chem. Eng. J.*, 2012, 209, 325-333.
3. O. H. Elsayed-Ali, T. Abdel-Fattah and H. E. Elsayed-Ali, *J. Hazard. Mater.*, 2011, 185, 1550-1557.
4. M. M. Matlock, B. S. Howerton and D. A. Atwood, *Water Res.*, 2002, 36, 4757-4764.
5. N. Meunier, P. Drogui, C. Montané, R. Hausler, G. Mercier and J.-F. Blais, *J. Hazard. Mater.*, 2006, 137, 581-590.
6. T. R. Harper and N. W. Kingham, *Water Environ. Res.*, 1992, 64, 200-203.
7. M. Marcucci, G. Ciardelli, A. Matteucci, L. Ranieri and M. Russo, *Desalination*, 2002, 149, 137-143.
8. B. Van Der Bruggen, C. Vandecasteele, T. Van Gestel, W. Doyen and R. Leysen, *Environ. Prog.*, 2003, 22, 46-56.
9. H. Ozaki, K. Sharma and W. Saktaywin, *Desalination*, 2002, 144, 287-294.
10. L. Di Palma, P. Ferrantelli, C. Merli and E. Petrucci, *Waste Manage.*, 2002, 22, 951-955.
11. A. Chianese, R. Ranauro and N. Verdone, *Water Res.*, 1999, 33, 647-652.
12. J. B. Brower, R. L. Ryan and M. Pazirandeh, *Environ. Sci. Technol.*, 1997, 31, 2910-2914.
13. A. Dąbrowski, Z. Hubicki, P. Podkościelny and E. Robens, *Chemosphere*, 2004, 56, 91-106.
14. R. R. Gadde and H. A. Laitinen, *Anal. Chem.*, 1974, 46, 2022-2026.
15. A. Demirbas, *J. Hazard. Mater.*, 2008, 157, 220-229.
16. P. S. Keng, S. L. Lee, S. T. Ha, Y. T. Hung and S. T. Ong, *Environ. Chem. Lett.*, 2014, 12, 15-25.
17. H. Yamaguchi, R. Higasida, M. Higuchi and I. Sakata, *J. Appl. Polym. Sci.*, 1992, 45, 1463-1472.
18. P. Miretzky, A. Saralegui and A. Fernández Cirelli, *Chemosphere*, 2006, 62, 247-254.
19. M. Sprynskyy, B. Buszewski, A. P. Terzyk and J. Namieśnik, *J. Colloid Interface Sci.*, 2006, 304, 21-28.
20. D. Sud, G. Mahajan and M. P. Kaur, *Bioresour. Technol.*, 2008, 99, 6017-6027.
21. L. Bois, A. Bonhommé, A. Ribes, B. Pais, G. Raffin and F. Tessier, *Colloid Surf. A-Physicochem. Eng. Asp.*, 2003, 221, 221-230.
22. D. W. O'Connell, C. Birkinshaw and T. F. O'Dwyer, *Bioresour. Technol.*, 2008, 99, 6709-6724.
23. S. Babel and T. A. Kurniawan, *J. Hazard. Mater.*, 2003, 97, 219-243.
24. Y. H. Wang, S. H. Lin and R. S. Juang, *J. Hazard. Mater.*, 2003, 102, 291-302.
25. W. S. Wan Ngah and M. A. K. M. Hanafiah, *Bioresour. Technol.*, 2008, 99, 3935-3948.
26. M. L. Huggins, *Macromolecules*, 1977, 10, 893-898.
27. C. Barba, S. Mendez, A. Roddick-Lanzilotta, R. Kelly, J. L. Parra and L. Coderch, *J. Cosmet. Sci.*, 2007, 58, 99-107.
28. S. Reichl, *Biomaterials*, 2009, 30, 6854-6866.
29. B. Srinivasan, R. Kumar, K. Shanmugam, U. T. Sivagnam, N. P. Reddy and P. K. Sehgal, *J. Biomed. Mater. Res. Part B-Appl. Biomater.*, 2010, 92B, 5-12.
30. A. Vasconcelos, G. Freddi and A. Cavaco-Paulo, *Biomacromolecules*, 2008, 9, 1299-1305.
31. Q. M. Li, L. J. Zhu, R. G. Liu, D. Huang, X. Jin, N. Che, Z. Li, X. Z. Qu, H. L. Kang and Y. Huang, *J. Mater. Chem.*, 2012, 22, 19964-19973.
32. M. Brebu and I. Spiridon, *J. Anal. Appl. Pyrolysis*, 2011, 91, 288-295.
33. E. Salminen and J. Rintala, *Bioresour. Technol.*, 2002, 83, 13-26.
34. W. F. Schmidt, presented in part at the Proceedings of the National Poultry Waste Management Symposium, Oct. 19-22, 1998.
35. D. Balkose and H. Baltacioglu, *J. Chem. Technol. Biotechnol.*, 1992, 54, 393-397.

36. P. Kar and M. Misra, *J. Chem. Technol. Biotechnol.*, 2004, 79, 1313-1319.
37. D. Touaibia and B. Benayada, *Desalination*, 2005, 186, 75-80.
38. A. Aluigi, C. Tonetti, C. Vineis, C. Tonin, R. Casasola and F. Ferrero, *J. Biobased Mater. Bioenergy*, 2012, 6, 230-236.
39. Y. Sekimoto, T. Okiharu, H. Nakajima, T. Fujii, K. Shirai and H. Moriwaki, *Environ. Sci. Pollut. Res.*, 2013, 20, 6531-6538.
40. Q. Wang, G. Jin, X. Fan, X. Zhao, L. Cui and P. Wang, *Appl. Biochem. Biotechnol.*, 2010, 160, 2486-2497.
41. M. Liouni, C. Touloupis, N. Hadjichristidis, S. Karvounis and E. Varriano-Marston, *J. Appl. Polym. Sci.*, 1992, 45, 2199-2205.
42. M. Ranjbar-Mohammadi, M. Arami, H. Bahrami, F. Mazaheri and N. M. Mahmoodi, *Colloid Surf. B-Biointerfaces*, 2010, 76, 397-403.
43. M. Niu, X. Liu, J. Dai, W. Hou, L. Wei and B. Xu, *Spectroc. Acta Pt. A-Molec. Biomolec. Spectr.*, 2012, 86, 289-293.
44. M. Periolatto, F. Ferrero, C. Vineis and F. Rombaldoni, *Carbohydr. Polym.*, 2013, 98, 624-629.
45. M. Morita, M. Higuchi and I. Sakata, *J. Appl. Polym. Sci.*, 1987, 34, 1013-1023.
46. C. Kantipuly, S. Katragadda, A. Chow and H. D. Gesser, *Talanta*, 1990, 37, 491-517.
47. P. A. Kavaklı and O. Güven, *J. Appl. Polym. Sci.*, 2004, 93, 1705-1710.
48. W. W. Li, R. G. Liu, H. L. Kang, Y. M. Sun, F. Y. Dong and Y. Huang, *Polym. Chem.*, 2013, 4, 2556-2563.
49. Y. S. Ho and G. McKay, *Process Biochem.*, 1999, 34, 451-465.
50. O. Bizerea Spiridon and L. Pitulice, *Environ Sci Pollut Res Int*, 2014, 21, 7236-7237.
51. Y. S. Ho, *J Hazard Mater*, 2006, 136, 681-689.
52. Y. S. Ho, *Environ Sci Pollut Res Int*, 2014, 21, 7234-7235.
53. Y. Tian, M. Wu, R. G. Liu, Y. X. Li, D. Q. Wang, J. J. Tan, R. C. Wu and Y. Huang, *Carbohydr. Polym.*, 2011, 83, 743-748.
54. N. Ünlü and M. Ersoz, *J. Hazard. Mater.*, 2006, 136, 272-280.
55. P. L. Smedley and D. G. Kinniburgh, *Appl. Geochem.*, 2002, 17, 517-568.
56. L. D. Meng, F. Q. Wang, J. P. Li, Y. Tian, M. Wu, D. Y. Wu, S. Kuga and Y. Huang, *Acta Polym. Sin.*, 2014, 1070-1077.

Journal Name

RSCPublishing

ARTICLE

TOC Graphic

Wool graft polyacrylamidoxime as the adsorbent for adsorption both cationic and anionic toxic ions from aqueous solutions†

Chun Cao, Hongliang Kang, Ning Che, Zhijing Liu, Pingping Li, Chao Zhang, Weiwei Li, Yong Huang, Ruigang Liu

Wool graft polyacrylamidoxime (W-*g*-PAO) was synthesized using coarse wool as the raw keratin material. The W-*g*-PAO can be used a cheap and excellent adsorbent for the removal of both cationic and anionic toxic ions from waste water. The approach can be extended to the modification of other waste raw keratin materials and used them as the blocks for the fabrication of functional materials.